همایش یافته های نوین در هوافضا و علوم وابسته

Modern Achievements on Aerospace and Related Sciences

تابستان ۱۳۹۲- تهران دانشکده علوم و فنون دانشگاه تهران

وب سایت همایش: AeroMech.ir

گواهی پذیرش مقاله

کد مقاله: HN10102870050

بدینوسیله گواهی می شود مقاله جناب آقای میلاد کاظمیان

با عنوان "Assessment of nano-metal additives in turbulent flow on two different solid rocket motor configurations"

" به همایش یافته های نوین در هوا فضا و علوم وابسته ارسال و پس از اوزیابی علی بصورت **پوستر** مورد پذیرش قرار گرفته است. توفیق روزافزون ایشان را در پیشبرد علم و فناوری کشور عزیزمان آرزومندیم.

نگارندگان به ترتیب اسامی: M. Kazemian, M. H. DJavareshkian

دکتر محمدحسین صبا

رئیس همایش

نشانی دبیرخانه: تهران- انتهای کارگر شمالی، بعد از پل شهید حکیم، دانشکده مکانیک، دانشگاه تهران- انتهای شماره ۱۰۲ پست الکترونیک: [illegible] تلفن دبیرخانه: ۰۹۱۰۱۴۰۱۰۶۴ فاکس: ۰۲۱۸۹۷۷۶۹۲۱

Assessment of nano-metal additives in turbulent flow on two different solid rocket motor configurations

Authors: M. Kazemian*[1], M. H. DJavareshkian[2]

Affiliations:

[1] Master of Aerospace Engineering, Propulsion Trend, Mechanical Engineering Department, Engineering Faculty, Ferdowsi University of Mashhad, Iran

[2] PhD of Aerospace Engineering, Associate Professor, Mechanical Engineering Department, Engineering Faculty, Ferdowsi University of Mashhad, Iran

* Correspondence Writer: email: kazemian.milad@gmail.com tell: +989153128735

Abstract:

In this work a density-based numerical modeling for internal ballistic parameters of solid rocket motors is developed. The replacement of propellant surface is modeled by dynamic mesh method. The effect of addition of three different types of nano-metal additives is investigated while the erosion phenomenon is considered. These parameters are tested for a nozzle less and a rocket with convergent- divergent nozzle. The achieved results show that regression rate of propellant surface for a rocket with nozzle is more significant, also amongst the different turbulent models the k-w SST model is more compatible with the physical condition.

Introduction:

Solid propellant is a self-sustaining combustible material containing both fuel and oxidizer in a solid state. In composite solid propellant, the oxidizer is a solid crystal particle of various sizes that is mixed into long hydrocarbon chains that are polymerized into rubber providing the fuel. The most common oxidizer crystal used in composite propellant is ammonium per chlorate (AP).

Tailoring propellants is a common goal in the propellant community that involves adjusting the propellant formulation or the addition of additives (*1*).

Through the addition of nano-scale metal oxide additives to composite solid propellant, it is possible to modify burning rate and achieve propellant tailoring (*2*). Controlling the composition, morphology and amount of these additives in the formulation of solid propellant allows the propulsion community to develop propellants with specific combustion characteristics. Such additives at mass loadings of 1% or even less can modify propellant in several ways including affecting material properties, partaking in the combustion process, or acting as catalysts. A characterization of the effects of these additives in propellant combustion can be favorable for affecting the combustion process through catalytic activity (*3*). Nano particles can be synthesized from the ground up to have specific surface chemistry and crystal structure. Chaturvedi et al. also worked on nano catalysts in order to improve

burning characteristics of a solid propellant (*4*). In addition to propellant properties it is needed to deal with phenomenon which happen in closed flow. Balable et al. studied a 2-D adiabatic compressible flow, wall shear stress and static pressure, separation point in order to compare turbulence models (*5*). Ghassemi et al. studied thermo dynamical aspects of magnesium additive on a solid rocket motor (SRM) (*6*). Maggi et.al focused on effects of metal and hydrid additives on burning rate and internal ballistic parameters of solid rockets (*7-9*). Zhang et al. have been modeled the erosion and its effects on internal ballistics of a solid rocket motor (*10*).

In spite of various researches on SRMs there is little knowledge about turbulence modeling of SRMs. In this study five different turbulence model, three Nano-additives and nozzle effect are investigated in conditions where erosion is considered.

Physical model:

A cylindrical inner burning grain connected with a convergent-divergent nozzle and a nozzle less one has been simulated. Chemical reactions are neglected but inlet fluxes are equal in gas Specifications, velocity, direction and magnitude to a real case fluxes. Figure 1 shows boundary conditions. Inner surface of grin considered as mass flow inlet which deforms with a dynamic mesh technique so propellant east and combustion chamber's west wall are assumed as deforming walls. It is considered hot gases come through the mass flow inlet boundary. As we know Convergent-divergent nozzle outlet is supersonic so it's considered the pressure outlet.

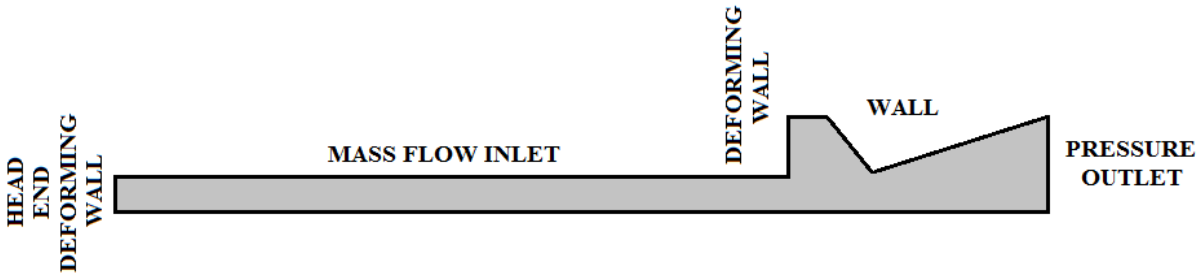

Figure 1: Boundary Conditions of Conv. - Div. Nozzle Rocket

As dynamic mesh had been used to simulate propellant regression the Tri- mesh style is access to split the solution domain. Nozzle throat is the most critical zone so the grid has been fined there. Figure 2 shows the boundary conditions for a nozzle less case, descriptions are same unless nozzle explanation.

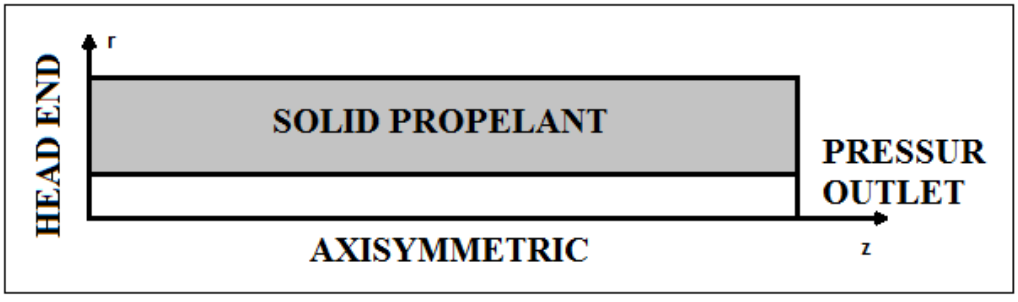

Figure 2: Boundary Conditions of Nozzle-less Rocket

Table 1 shows some geometrical information about the rocket.

Table 1: Geometrical Information

$L_{chamber}$	0.835 m
R_{out}	0.03175 m
R_{in}	0.0105 m
R_{throat}(for nozzle one)	0.01015 m

Mathematical model:

For modeling of problem firstly the vector form of equation is used. The density-based solver numerically solves the governing equations of continuity, momentum, and energy and species transport. For incompressible flows, regardless of the fluid velocity, because acoustic waves travel infinitely fast in an incompressible fluid (speed of sound is infinite). The numerical stiffness of the equations under these conditions results in poor convergence rates. This difficulty is overcome in density-based solver by employing a technique called (time-derivative) preconditioning (*11*). The inviscid flux vector is evaluated by a standard upwind, flux-difference splitting (*12*). The demonstration of these stages is stated in this sub-section.

Governing Equations in Vector Form:

The system of governing equations for a single-component fluid, written to describe the mean flow properties, is cast in integral Cartesian form for an arbitrary control volume V with differential surface area dA as follows:

$$\frac{\partial}{\partial t}\int_{\mathrm{V}} W d\mathrm{V} + \oint (F - G) dA = \int_{V} H dV \qquad (1)$$

Where

$$W = \begin{pmatrix} \rho \\ \rho u \\ \rho v \\ \rho w \\ \rho E \end{pmatrix}, \qquad F = \begin{pmatrix} \rho v \\ \rho uv + Pi \\ \rho vv + Pj \\ \rho uw + Pk \\ \rho vE + Pv \end{pmatrix}, \qquad G = \begin{pmatrix} 0 \\ \tau_{xi} \\ \tau_{yi} \\ \tau_{zi} \\ \tau_{ij} v_j + q \end{pmatrix} \qquad (2)$$

And the vector H contains source terms such as body forces and energy sources.

Here ρ,v,E, and P are the density, velocity, total energy per unit mass, and pressure of the fluid, respectively. τ is the viscous stress tensor, and q is the heat flux.

Total energy E is related to the total enthalpy H by

$$E = H - {}^{p}/_{\rho} \qquad (3)$$

Where

$$H = h + |v|^2/2 \quad (4)$$

The Navier-Stokes equations as expressed in Equation 1 become (numerically) very stiff at low Mach number due to the disparity between the fluid velocity v and the acoustic speed c (speed of sound). This is also true.

Preconditioning:

Time-derivative preconditioning modifies the time-derivative term in Equation 1 by pre-multiplying it with a preconditioning matrix. This has the effect of re-scaling the acoustic speed (Eigen-value) of the system of equations being solved in order to alleviate the numerical stiffness encountered in low Mach numbers and incompressible flow.

Derivation of the preconditioning matrix begins by transforming the dependent variable in Equation 1 from conserved quantities W to primitive variables Q using the chain-rule as follows:

$$\frac{\partial W}{\partial Q}\frac{\partial}{\partial t}\int_V QdV + \oint (F - G)dA = \int_V HdV \quad (5)$$

Where Q is the vector $\{p, u, v, w, T\}^T$ and the Jacobian $\frac{\partial W}{\partial Q}$ is given by

$$\frac{\partial W}{\partial Q} = \begin{bmatrix} \rho_p & 0 & 0 & 0 & \rho_T \\ \rho_p u & \rho & 0 & 0 & \rho_T u \\ \rho_p v & 0 & \rho & 0 & \rho_T v \\ \rho_p w & 0 & 0 & \rho & \rho_T w \\ \rho_p H - \delta & \rho u & \rho v & \rho w & \rho_T H + \rho C_p \end{bmatrix} \quad (6)$$

Where

$$\rho_P = \frac{\partial \rho}{\partial p}\Big|_T, \rho_T = \frac{\partial \rho}{\partial T}\Big|_p \quad (7)$$

And δ = 1 for an ideal gas and δ = 0 for an incompressible fluid.

The choice of primitive variables Q as dependent variables is desirable for several reasons. First, it is a natural choice when solving incompressible flows. Second, when we use second-order accuracy we need to reconstruct Q rather than W in order to obtain more accurate velocity and temperature gradients in viscous fluxes, and pressure gradients in inviscid fluxes. And finally, the choice of pressure as a dependent variable allows the propagation of acoustic waves in the system to be singled out (*13*).

We precondition the system by replacing the Jacobin matrix $\frac{\partial W}{\partial Q}$ (Equation 6) with the preconditioning matrix Γ so that the preconditioned system in conservation form becomes

$$\Gamma\frac{\partial}{\partial t}\int_V QdV + \oint (F - G)dA = \int_V HdV \quad (8)$$

Where

$$\Gamma = \begin{bmatrix} \Theta & 0 & 0 & 0 & \rho_T \\ \Theta u & \rho & 0 & 0 & \rho_T u \\ \Theta v & 0 & \rho & 0 & \rho_T v \\ \Theta w & 0 & 0 & \rho & \rho_T w \\ \Theta H - \delta & \rho u & \rho v & \rho w & \rho_T H + \rho C_p \end{bmatrix} \quad (9)$$

The parameter Θ is given by

$$\Theta = \left(\frac{1}{U_r^2} - \frac{\rho_T}{\rho C_p}\right) \quad (10)$$

The reference velocity U_r appearing in Equation 10 is chosen locally such that the eigenvalues of the system remain well conditioned with respect to the convective and diffusive time scales (*14*).

The resultant Eigen-values of the preconditioned system (Equation 8) are given by

$$u, u, u, u', u' + c', u' - c' \quad (11)$$

$$u = v.\hat{n} \quad (12)$$

$$u' = u(1 - \alpha) \quad (13)$$

$$c' = \sqrt{\alpha^2 u^2 + U_r^2} \quad (14)$$

$$\alpha = (1 - \beta U_r^2)/2 \quad (15)$$

$$\beta = \left(\rho_P + \frac{\rho_T}{\rho C_P}\right) \quad (16)$$

For an ideal gas, $\beta = (\gamma RT)^{-1} = 1/c^2$. Thus, when $U_r = c$ (at sonic speeds and above), α=0 and the eigenvalues of the preconditioned system take their traditional form, u±c. At low speed when$U_r \to 0$ and $\alpha \to 1/2$, all Eigen-values become of the same order as u. For constant-density flows, β=0 and α=1/2 regardless of the values of U_r. As long as the reference velocity is of the same order as the local velocity, all eigenvalues remain of the order u. Thus, the eigenvalues of the preconditioned system remain well conditioned at all speeds.

Note that the non-preconditioned Navier-Stokes equations are recovered exactly from Equation 8 by setting $1/U_r^2$ to ρ_p, the derivative of density with respect to pressure. In this case Γ reduces exactly to the Jacobin $\frac{\partial W}{\partial Q}$.

Although Equation 8 is conservative in the steady state, it is not, in a strict sense, conservative for time-dependent flows. This is not a problem, however, since the preconditioning has already destroyed the time accuracy of the equations and we will not employ them in this form for unsteady calculations.

For unsteady calculations, an unsteady preconditioning is available when the dual-time stepping method is used. The unsteady preconditioning enhances the solution accuracy by improving the scaling of the artificial dissipation and maximizes the efficiency by optimizing the number of sub-iterations required at each physical time step (15). For low Mach number flows in particular, for both low frequency problems (large time steps) and high frequency problems (small time step), significant savings in computational time are possible when compared with the non-preconditioned case.

The unsteady preconditioning adapts the level of preconditioning based on the user specified time-step and on the local advective and acoustic time scales of the flow. For acoustic problems, the physical time-step size is small as it is based on the acoustic CFL number. In this case the preconditioning parameter U_r^2 will approach c^2, which in effect will turn off the low-Mach preconditioning almost completely. For advection dominated problems, like the transport of turbulent vertical structures, etc., the physical time-step is large as it is based on the particle CFL number. The corresponding unsteady preconditioning parameter U_r^2 will then approach u^2, which corresponds to the steady preconditioning choice. For intermediate

physical time-step sizes, the unsteady preconditioning parameter will be adapted to provide optimum convergence efficiency of the pseudo-time iterations and accurate scaling of the artificial dissipation terms, regardless of the choice of the physical time step.

Roe Flux-Difference Splitting Scheme:

The inviscid flux vector F appearing in Equation 8 is evaluated by a standard upwind, flux-difference splitting (*12*). This approach acknowledges that the flux vector F contains characteristic information propagating through the domain with speed and direction according to the Eigen-values of the system. By splitting F into parts, where each part contains information traveling in a particular direction (i.e., characteristic information), and upwind differencing the split fluxes in a manner consistent with their corresponding Eigen-values, we obtain the following expression for the discrete flux at each face:

$$F = \frac{1}{2}(F_R + F_L) - \frac{1}{2}\Gamma\left|\hat{A}\right|\delta Q \quad (17)$$

Here δQ is the spatial difference $Q_R - Q_L$. The fluxes $F_{\mathrm{R}} = \mathrm{F}(\mathrm{Q_R})$ and $F_{\mathrm{L}} = \mathrm{F}(\mathrm{Q_L})$ are computed using the (reconstructed) solution vectors Q_R and Q_{L} on the "right" and "left" side of the face. The matrix $\left|\hat{A}\right|$ is defined by

$$\left|\hat{A}\right| = \mathrm{M}|\Lambda|\mathrm{M}^{-1} \quad (18)$$

Where Λ is the diagonal matrix of Eigen-values and M is the modal matrix Γ^{-1}A, where A is the inviscid flux Jacobin $\partial F/\partial Q$.

For the non-preconditioned system (and an ideal gas) Equation 17 reduces to Roe's flux-difference splitting (*12*) when Roe-averaged values are used to evaluate $\Gamma\left|\hat{A}\right|$. At present, arithmetic averaging of states Q_R and Q_{L} is used.

In its current form, Equation 17 can be viewed as a second-order central difference plus added matrix dissipation. The added matrix dissipation term is not only responsible for producing an upwind convected variables, and of pressure and flux velocity in supersonic flow, but it also provides the pressure-velocity coupling required for stability and efficient convergence of low-speed and incompressible flows.

General solution:

The density-based solver solves the governing equations of continuity, momentum, and (where appropriate) energy and species transport simultaneously as a set, or vector, of equations. Governing equations for additional scalars will be solved sequentially (i.e., segregated from one another and from the coupled set). Two algorithms are available for solving the coupled set of equations, the coupled-explicit formulation and the coupled-implicit formulation. Each iteration consists of the steps which outlined below:

1. Update the fluid properties based on the current solution. (If the calculation has just begun, the fluid properties will be updated based on the initialized solution.)
2. Solve the continuity, momentum, and (where appropriate) energy and species equations simultaneously.
3. Where appropriate, solve equations for scalars such as turbulence and radiation using the previously updated values of the other variables.

4. When interphase coupling is to be included, update the source terms in the appropriate continuous phase equations with a discrete phase trajectory calculation.
5. Check for convergence of the equation set.

These steps are continued until the convergence criteria are met.

Results and Discussions:

Solid fuel rockets are mostly considered as porous tubes in which gases are injected through walls. Compressibility effects could be considered depends on injecting velocity and chamber dimension. It is neglected in some researches. A 2-D axi-symmetric simulation is used to model the internal ballistics of the rocket by a density based solver and by means of a code in order to simulate propellant burning face regression.

Four formulations had been tested in this research to study the effect of nano additions on burning and regression rates.

Table 2 shows ballistic coefficients for these propellants.

Table 2: Ballistic Coefficients

Formulation	a	n
HTPB-AP	4.29	0.3425
HTPB-AP-Ti	4.11	0.4724
HTPB-AP-Ti-Al	4.44	0.4517
HTPB-AP-Ti-Fe	5.14	0.4103

Note that Pressure, P, is in units of MPa, and burning rate, r, is in units of mm/s.

Also, the effect of erosion on burning rate has been studied. Finally five different turbulence models have been compared in order to find the best perturbation method.

Three different grids had been generated to prove mesh independence. Figure 3 shows average pressure along the symmetry axis during burning time for three different grids with 667, 1900 and 4917 cells. As it is obvious 1900 and 4917 cells mesh have same and good adaption so in order to decreasing solution costs it is decided to use 1900 cells grid to solve the flow inside the domain.

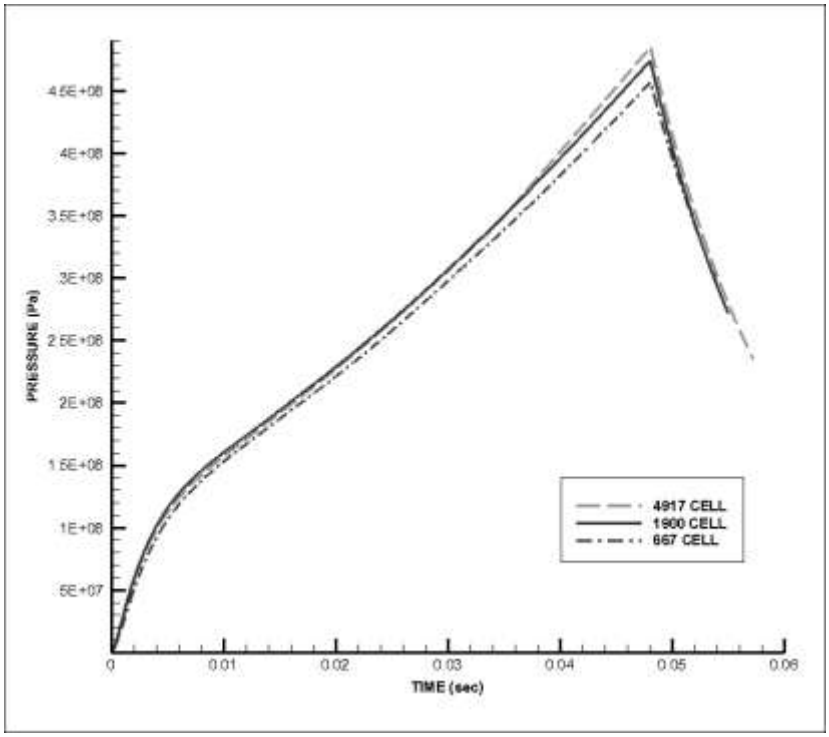

Figure 3: Grid Check and Mesh Independency

Gottelieb (*16*) had used 1-D invicid Euler formulation to simulate a solid rocket motor. Figure 4 shows very good adaptation between current work and published research. This figure presents average pressure along symmetry axis Vs burning time, pressure is in unit of Pascal and time is in unit of second. As current study utilizing a 2-D viscose Navier-Stocks equations and considering wall effects in turbulence model there is slight differences but it is negligible.

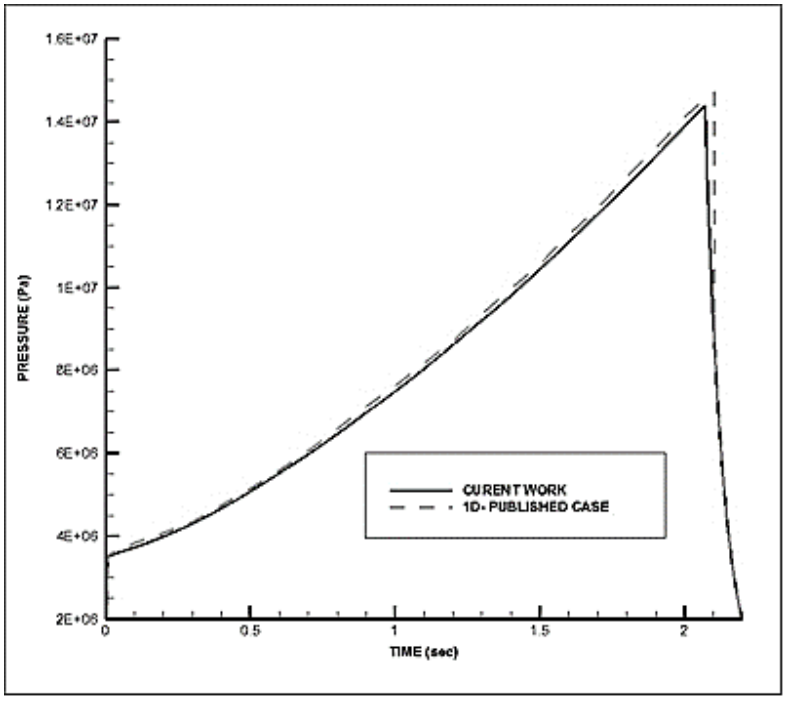

Figure 4: Validation with Previous Works

The solver needs an initial value to start the solution; in this case pressure and temperature are equal to atmospheric condition through whole domain. When a rocket starts to operate, burnet gases come into combustion chamber through propellant surface, for the nozzle case within a short time throat become choked and chamber pressure start to rise, as it is an inner burning grin and burning rate is connected with pressure they superpose their effects and chamber pressure raises. the code reads current position of propellant cells surface and pressure of them, calculates the burning rate and estimates the velocity of entrance gases and amount of displacement of inlet boundary, there is a condition in code which compares grin web with predefined magnitude to stop moving inlet face and flux generation when propellant burns out, at this time burning process had been finished and there is just pressure discharge from combustion chamber to atmosphere. Figure 5 shows this process for four different propellants in. The mixture of Titania and nano Iron shows better performance and higher chamber pressure during the program run in both case. These additives are caused propellant to burn in higher rates, produce higher chamber pressure and finishes sooner in time. These effects cause an increase in the specific impulse. In this figure average pressure along symmetry axis is plotted. Figure 6 shows same story for nozzle less case, in order to show variation of pressure for certain times, in this figure pressure along symmetry axis is plotted for certain propellant and four certain time.

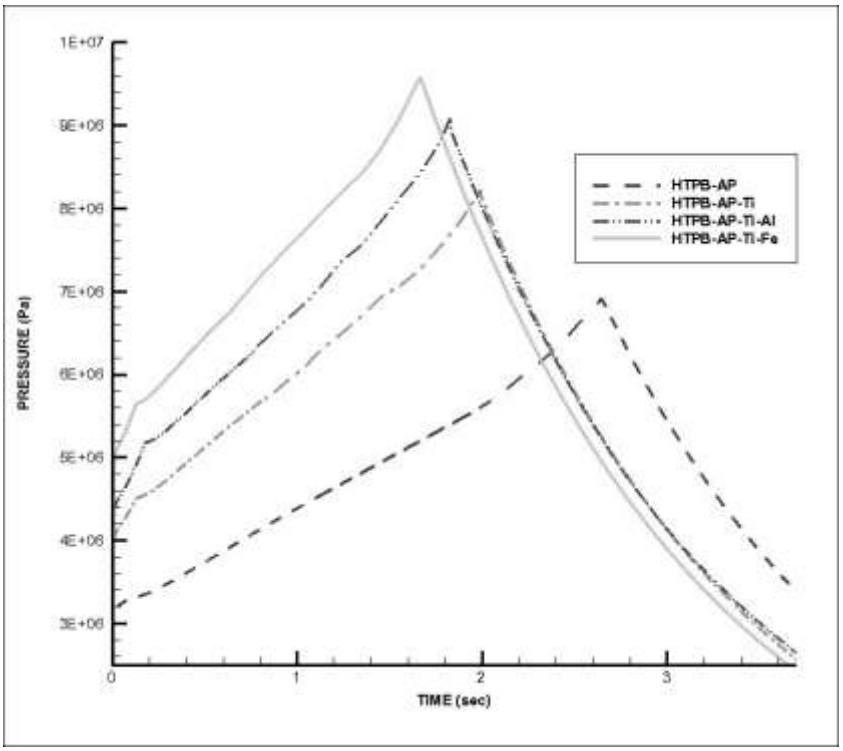

Figure 5: Average Pressure along Symmetry Axis vs. Burning Time (Con. –Div. Rocket)

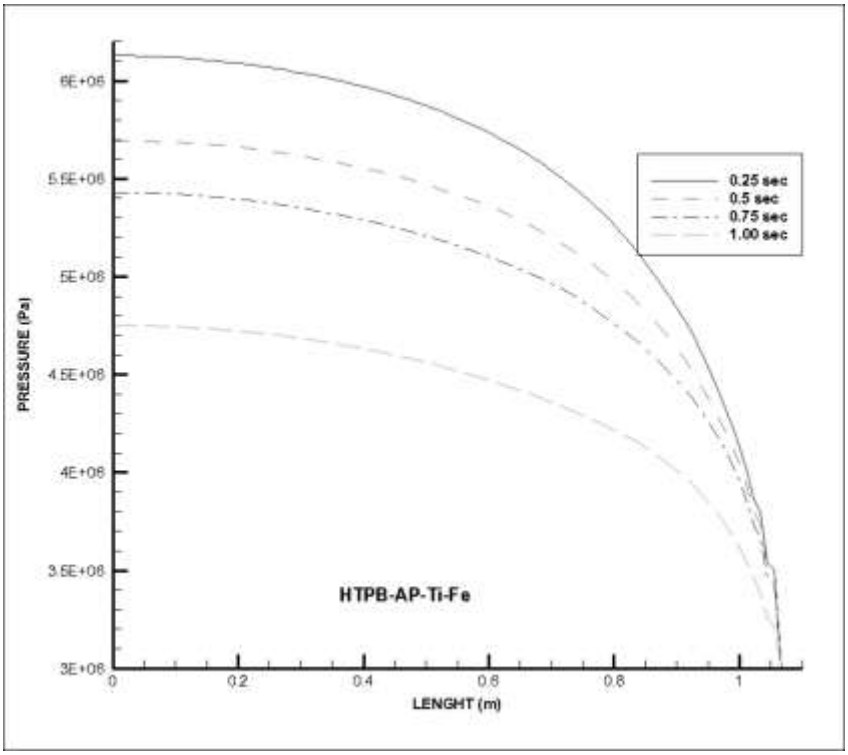

Figure 6: Average Pressure along Symmetry Axis vs. Burning Time (Nozzle-less Rocket)

Erosion is a Phenomenon which occurs in any combustion process but it is more important in high aspect ratio rockets where a high aspect ratio rocket is a rocket with high length to diameter ratio. In an ideal rocket it is assumed that the velocity is perpendicular to surface and it is parallel to rocket axis in the centre, when diameter becomes much more less velocity finds horizontal coefficient propellant and causes erosion along that mostly at the end of grin. Reference (*17*) gives a formula to simulate the effect of erosion. Figure 7 and 8 show average pressure and flux along the symmetry axis during burning time. It is obvious that erosion causes more burning rate and more pressure and less burning time. Figure 7 represents averaged pressure along axis Vs time. As it is obvious erosion causes chamber pressure rises to 8 mega Pascal at the beginning of burn process which is 1.6 times more. Figure 8 shows that erosion effects cause's 0.5 kg/s increase in average mass flux of inlet surface.

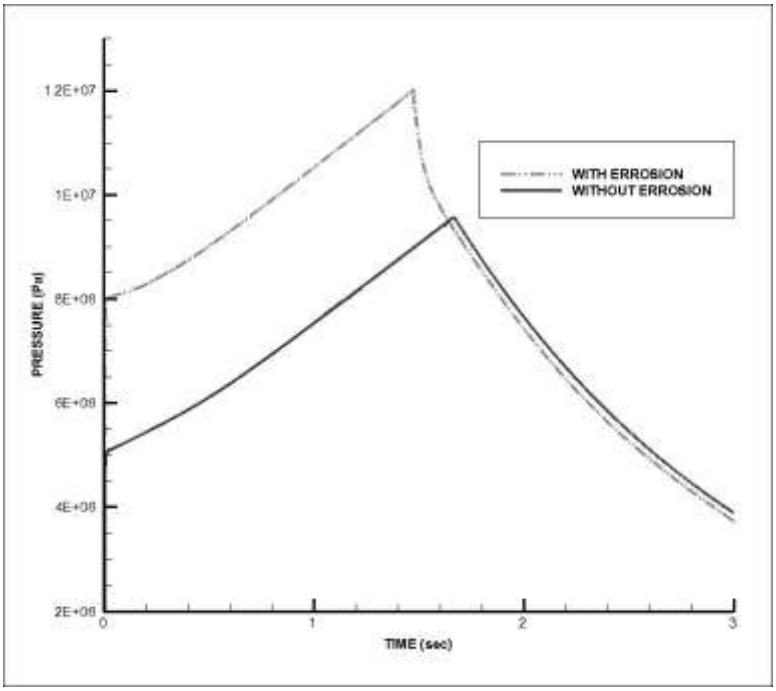

Figure 7: Average Pressure along the Symmetry Axis vs. Burning Time

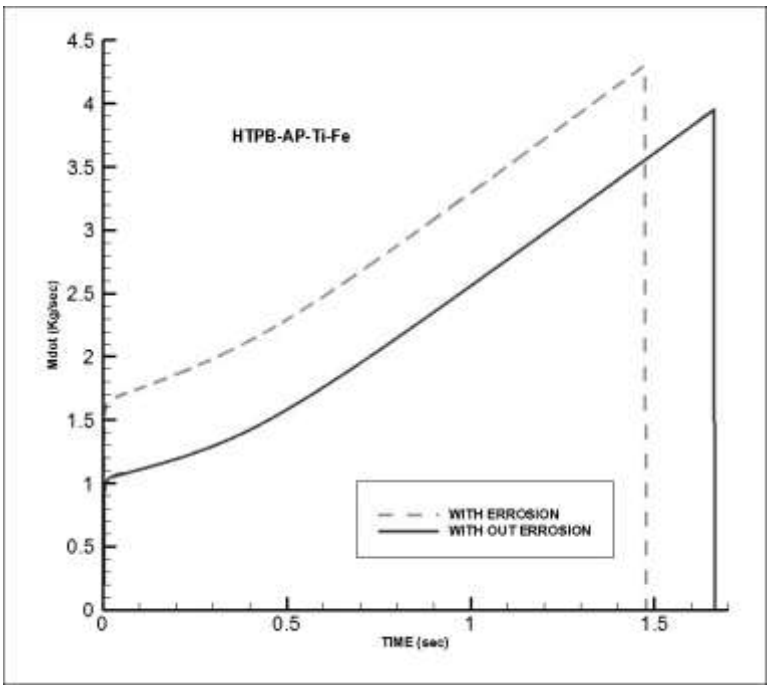

Figure 8: Average Flux along the Symmetry Axis vs. Burning Time

Figure 9 shows Mach number contour for HTPB-AP-Ti-Fe for time 1.26 second. Figure 9 shows a fully developed flow discharging into the atmosphere through the nozzle which Mach number at outlet reaches to 3.22.

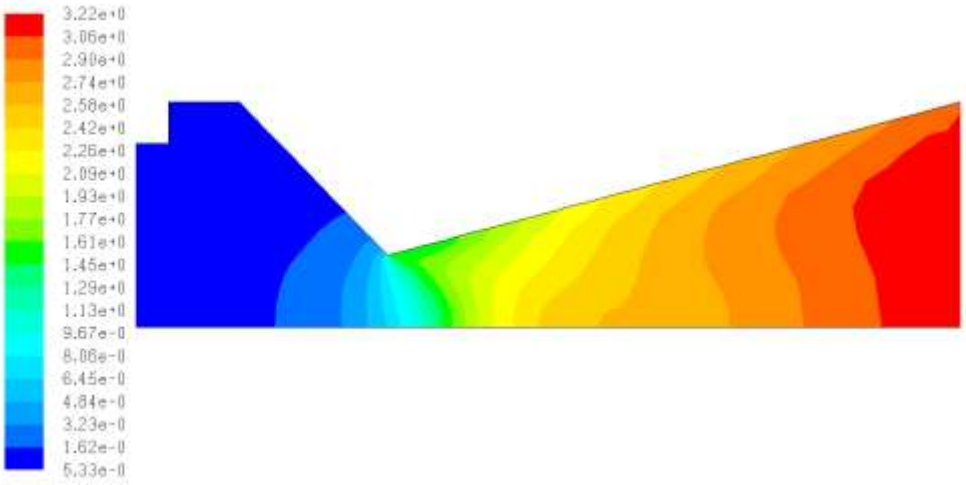

Figure 9: Mach-Number Contour for HTPB-AP-Ti-Fe for Time 1.26 sec.

Figure 10 and figure 11 show position of propellant surface during the time. As it is obvious in nozzle case (figure 10) the end part of grin is more affected because of chamber pressure and gas velocity but in figure 11, nozzle less case, as exhaust velocity is below sound velocity and pressure is lower the end part of the grin is less affected.

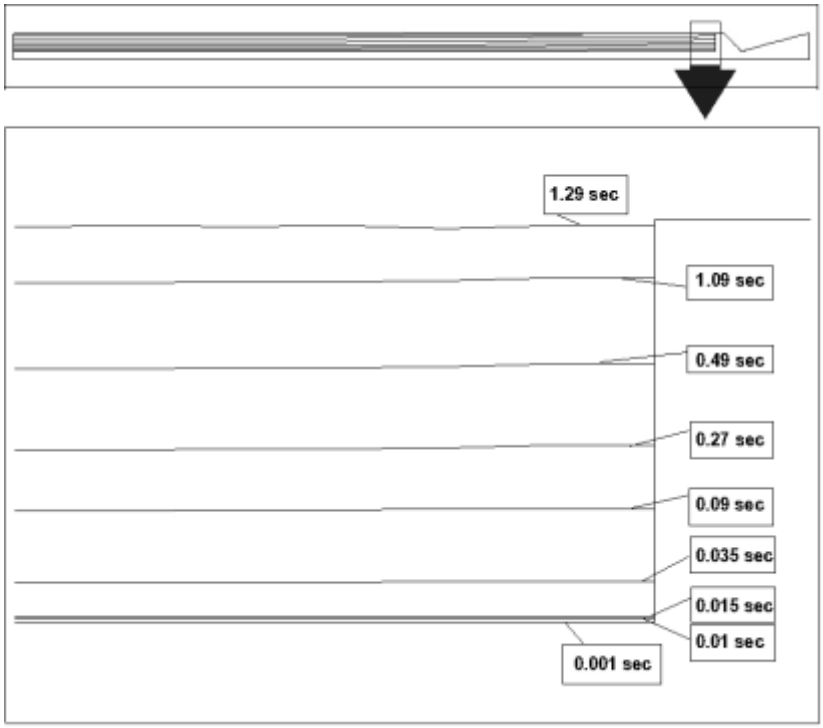

Figure 10: Position of Propellant Surface during the Time (Con. –Div. Rocket)

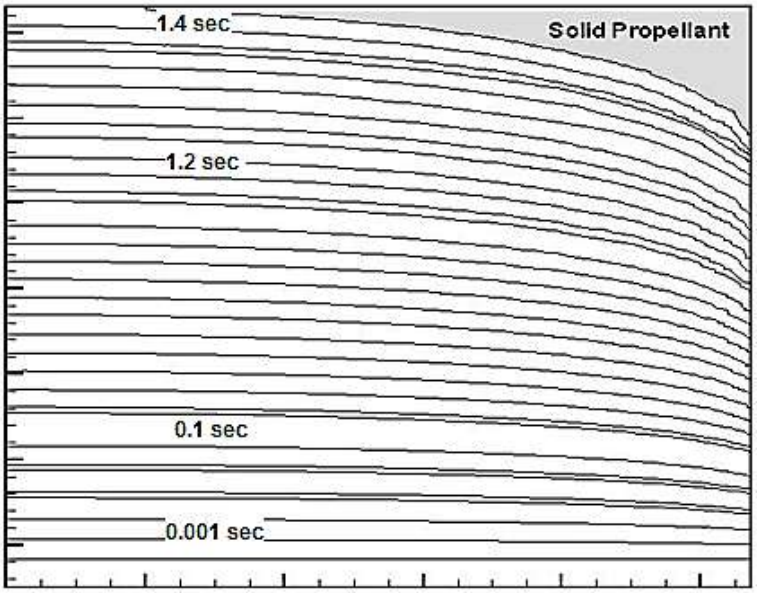

Figure 11: Position of Propellant Surface during the Time (Nozzle-less Rocket)

As Navier-Stocks viscose formulation is used, choosing a proper turbulence model to predict Reynolds shear stresses is very important. By studying the physics of current case we decide to use two equation models because of their abilities to cover high-low Reynolds flows. Figure 12 shows the same case which had run for five different turbulence models.

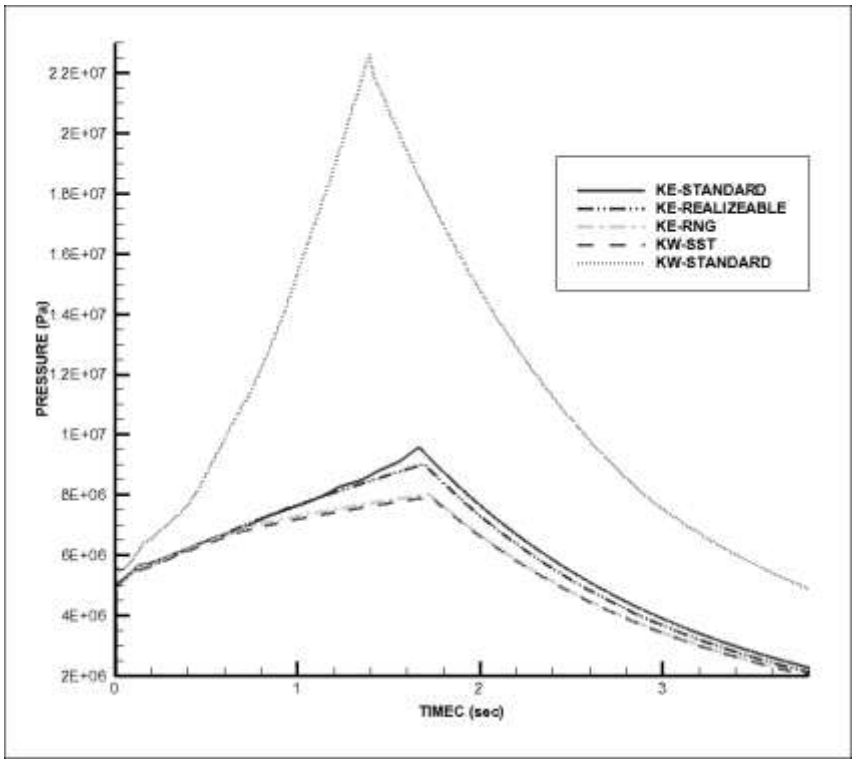

Figure 12: Compare of Different Turbulence Models

k-ε and k-ω models are developed by different assumption in order to cover flows by different Reynolds numbers. K-ε standard and Realizable are covering just high Reynolds numbers and k-ω standard covers just low Reynolds numbers so it is obvious that for this case, with high and low Reynolds area near axis and walls, we need a model which could cover both Reynolds numbers, so using k-ε RNG and k-ω SST which both have terms to cover high and low Reynolds regions lead us to reach same result as it shown in figure 12.

Conclusion:

In this modeling the investigation of effects of nano-metal additives, erosion and turbulent model in solid rocket motors is done. The main achieved results can be abbreviated as follows.

- Addition of nano-iron and titanium particles shows better behavior in internal ballistic parameters in both cases.
- The effects of erosion cannot be neglected in high aspect ratio SRM numerical modeling especially in nozzle case.
- Considering erosion is resulted to raise the chamber pressure from 8 to 12.8MPa.
- Propellant regression is different in these two cases, as velocity and pressure are less at end part of grin in nozzle less case, burning is fewer too.
- The Realizable and K-ε standard turbulent models are applicable in high Reynolds numbers while k-ω standard can be used in low Reynolds numbers.
- k-ε RNG and k-ω SST turbulent models are appropriate for total ranges of Reynolds numbers where the solution time is improved in the k-ω SST model.

References and Notes:

[1] NASA. Motor Propellant Development. Aerojet-General Corporation, Sacramento, California. report 260-SL-3. 1967.

[2] Stephens, M., Petersen, E., Carro, R., Reid, D., and Seal, S. Multi-Parameter Study of Nanoscale TiO2 and CeO2 Additives in Composite AP/HTPB Solid Propellants. Propellants, Explosives, Pyrotechnics. 35,143-152. 2010.

[3] Fujimura, K. and Miyake, A. The Effectof Specific Surface Area of TiO2 on the Thermal Decomposition of Ammonium Perchlorate. Journal of Thermal Analysis and Calorimetry. 99,27-31. 2009.

[4] Shalini Chaturvedi, Pragnesh N. Dave, N.K. Shah, "Applications of nano-catalyst in new era", Journal of Saudi Chemical Society 16, pp. 307–325, 2012.

[5] A. Balabel, A.M. Hegab, M. Nasr, Samy M. El-Behery, "Assessment of turbulence modeling for gas flow in two-dimensional convergent–divergent rocket nozzle", Applied Mathematical Modelling 35, PP. 3408–3422, 2011.

[6] Hojat Ghassemi, Hamidreza Farshi Fasih, "Propulsive characteristics of metal fuel-rich pyrotechnics in hydro-reactive motors", Aerospace Science and Technology, 2012.

[7] Filippo Maggi, Alessio Bandera, Luciano Galfetti, Luigi T. De Luca, Thomas L. Jackson, "Efficient solid rocket propulsion for access to space", Acta Astronautica 66, pp. 1563–1573, 2010.

[8] Filippo Maggi, Gabriela Gariani, Luciano Galfetti, Luigi T. DeLuca, "Theoretical analysis of hydrides in solid and hybrid rocket propulsion", inte rnational journal of hydrogen energy 37, pp. 1760-1769, 2012.
[9] Filippo Maggi, Stefano Dossi, Luigi T. DeLuca, "Combustion of metal agglomerates in a solid rocket core flow", Acta Astronautica, 2012.
[10] Ju Zhang, Thomas L. Jackson, "A model for erosive burning of homogeneous propellants", Combustion and Flame 157, pp. 397–407, 2010.
[11] J. M. Weiss and W. A. Smith. "Preconditioning Applied to Variable and Constant Density Flows." AIAA Journal, 33(11):2050-2057, November 1995.
[12] P. L. Roe. Characteristic based schemes for the Euler equations. *Annual Review of Fluid Mechanics*, 18:337-365, 1986.
[13] S. Venkateswaran, J. M. Weiss, and C. L. Merkle. Propulsion Related Flowfields Using the Preconditioned Navier-Stokes Equations. Technical Report AIAA-92-3437, AIAA/ASME/SAE/ASEE 28th Joint Propulsion Conference, Nashville, TN, July 1992.
[14] J. M. Weiss and W. A. Smith. Preconditioning Applied to Variable and Constant Density Flows. AIAA Journal, 33(11):2050-2057, November 1995.
[15] S. A. Pandya, S. Venkateswaran, and T. H. Pulliam. Implementation of dual-time procedures in overflow. Technical Report AIAA-2003-0072, American Institute of Aeronautics and Astronautics, 2003.
[16] J.J. Gottlieb and D.R. Greatrix, "numerical study of the effects of longitudinal acceleration on solid rocket motor internal ballistics", Journal of Fluid Engineering, Vol. 114, September 1992.
[17] Barrere, M. and et.al., Rocket Propulsion, Amsterdam, Elsevier,1960.